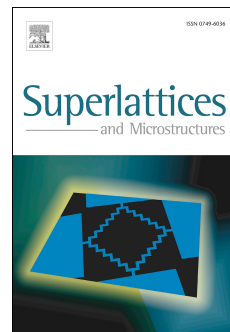


Accepted Manuscript

Ab-initio study of electronic and optical properties of biaxially deformed single-layer GeS

Khang D. Pham, Chuong V. Nguyen, Huynh V. Phuc, Tuan V. Vu, Nguyen V. Hieu, Bui D. Hoi, Le C. Nhan, Vo Q. Nha, Nguyen N. Hieu



PII: S0749-6036(18)30910-8

DOI: [10.1016/j.spmi.2018.06.013](https://doi.org/10.1016/j.spmi.2018.06.013)

Reference: YSPMI 5748

To appear in: *Superlattices and Microstructures*

Received Date: 3 May 2018

Revised Date: 6 June 2018

Accepted Date: 6 June 2018

Please cite this article as: K.D. Pham, C.V. Nguyen, H.V. Phuc, T.V. Vu, N.V. Hieu, B.D. Hoi, L.C. Nhan, V.Q. Nha, N.N. Hieu, Ab-initio study of electronic and optical properties of biaxially deformed single-layer GeS, *Superlattices and Microstructures* (2018), doi: 10.1016/j.spmi.2018.06.013.

This is a PDF file of an unedited manuscript that has been accepted for publication. As a service to our customers we are providing this early version of the manuscript. The manuscript will undergo copyediting, typesetting, and review of the resulting proof before it is published in its final form. Please note that during the production process errors may be discovered which could affect the content, and all legal disclaimers that apply to the journal pertain.

Highlights

- Single-layer GeS is an indirect band gap semiconductor of 1.82 eV at the equilibrium state
- Semiconductor-metal phase transition occurs in single-layer GeS at large compression biaxial strain
- Optical absorption of single-layer GeS is high in the range of the middle ultraviolet lights
- Effect of biaxial strain on optical spectra are only apparent in energy domain greater than 4 eV

Ab-initio study of electronic and optical properties of biaxially deformed single-layer GeS

Khang D. Pham^{a,b}, Chuong V. Nguyen^c, Huynh V. Phuc^d,
Tuan V. Vu^{e,f}, Nguyen V. Hieu^g, Bui D. Hoiⁱ, Le C. Nhan^h,
Vo Q. Nha^j, Nguyen N. Hieu^{k,*}

^a*Theoretical Physics Research Group, Advanced Institute of Materials Science,
Ton Duc Thang University, Ho Chi Minh City, Viet Nam*

^b*Faculty of Applied Sciences, Ton Duc Thang University, Ho Chi Minh City, Viet Nam*

^c*Department of Materials Science and Engineering, Le Quy Don Technical University, Ha
Noi, Viet Nam*

^d*Division of Theoretical Physics, Dong Thap University, Dong Thap, Viet Nam*

^e*Division of Computational Physics, Institute for Computational Science, Ton Duc Thang
University, Ho Chi Minh City, Viet Nam*

^f*Faculty of Electrical and Electronics Engineering, Ton Duc Thang University, Ho Chi
Minh City, Viet Nam*

^g*Department of Physics, University of Education, The University of Da Nang, Da Nang,
Viet Nam*

^h*Department of Environmental Sciences, Saigon University, Ho Chi Minh City, Viet Nam*

ⁱ*Department of Physics, University of Education, Hue University, Hue, Viet Nam*

^j*Department of Electrical Engineering, Quang Tri Branch, Hue University, Quang Tri,
Viet Nam*

^k*Institute of Research and Development, Duy Tan University, Da Nang, Viet Nam*

Abstract

In the present work, using density functional theory (DFT), we investigate the influence of biaxial strain ε_b on electronic and optical properties of single-layer GeS. Our DFT calculations show that single-layer GeS is a semiconducting material at equilibrium and semiconductor-metal phase transition may occur at large compression biaxial strain. The optical absorption of single-layer GeS is high in the range of the middle ultraviolet lights. Besides, the biaxial has a great impact on the optical spectra of single-layer GeS in the high energy domains. The semiconductor-metal phase transition and the computational results of the absorption of GeS can provide more useful information for applications in nanoelectromechanical and optoelectronic devices.

Key words: Deformed GeS, band structure, optical properties

1 Introduction

Graphene is one of the materials that has attracted much interest over the past decade due to its extraordinary physical properties. Synthesis of graphene successfully is an important milestone in the study of layered materials [1]. In parallel with graphene studies, many scientists have focused on the search for new layered materials [2] and heterostructures made by two-dimensional (2D) materials [3–6]. Recently, several layered materials have been successfully synthesized and initially applied in electronic technology, such as MoS₂ [7, 8], phosphorene [9, 10] or monochalcogenide nanosheets [11, 12]. Also, many theoretical studies focused on the layered transition metal dichalcogenides [13–15], phosphorene [16, 17] and

* Corresponding author. Tel.: +84-236-3827-111

Email addresses: phamdinhkhang@tdt.edu.vn (Khang D. Pham),
hieunn@duytan.edu.vn (Nguyen N. Hieu).

phosphorene-like two-dimensional single-layer binary IV-VI compounds [18–23]. In contrast to 2D graphene, a semiconductor with zero bandgap, phosphorene-like materials have large nature band gap and very high carrier mobility [24], which makes it convenient to apply them to electronic devices.

The bulk GeS has been investigated by both theoretically and experimentally for long time [25, 26] and GeS nanosheet has also recently been successfully synthesized [11, 27]. Based on the DFT calculations, Singh and Hennig predicted that single-layer GeS could be synthesized by common techniques such as molecular beam epitaxy or chemical vapor deposition because of its low formation energy [28]. Besides, previous theoretical calculations have confirmed that single-layer GeS is dynamically stable because there are no soft modes in its phonon spectrum [29]. In parallel with the experimental studies, the scientists also focused on theoretical studies on single-layer GeS. Single-layer GeS is an indirect bandgap semiconductor [30]. Quite recently, a short description of the band structure of single-layer GeS using a tight binding model has been made [31]. Also, several works have focused on electronic properties and optical characters of group IV single-layer monochalcogenide materials, including GeS [32–35]. Zhang and co-workers have investigated electronic transport properties of the GeS nanoribbons using non-equilibrium Green's function (NEGF) combined with DFT method [35]. Influence of a strain and an external electric field on electronic states of single-layer GeS has also been considered by first-principles calculations [29]. One can control the band gap of single-layer GeS by the mechanical strain [36, 37]. Also, it has been shown that the strain, especially biaxial strain, strongly affects the electronic properties of single-layer GeS. The biaxial strain can cause a semiconductor-metal phase transition [29, 38]. First-principles study also showed that the elastic strain can be modulated the ferroelectric polarization of single-layer GeS [22]. Also, Fei and co-workers have predicted that single-layer GeS is a ferroelectric material with

many promising applications in the devices [20]. Moreover, the optical spectra of single-layer GeS are very anisotropic [22], and it has excellent absorption in the range of ultraviolet lights [38] which is useful for applications in the optoelectronics. Besides, optical properties of single-layer group-IV monochalcogenides such as GeSe or GeTe have also been considered by different methods [34, 39–41]. Huang and co-worker showed that the bandgap of the single-layer GeX (X = S, Se, Te) reduces as the X atoms (chalcogenide atoms) when they changes from S to Te [38]. It means that the bandgap of single-layer GeS is bigger than that of GeSe. In this paper, we consider the influence of biaxial strain on electronic and optical properties of single-layer GeS by density functional theory (DFT).

2 Theoretical model and method

In the present work, we performed first-principles calculations for geometry and electronic properties of single-layer GeS using the Quantum Espresso code [42] with the generalized gradient approximations (GGA) of Perdew-Burke- Ernzerhof (PBE) functional [43, 44]. Whereas, the ion-electron interaction is treated with the projector augmented-wave (PAW) method. A cut-off of kinetic energy for plane-wave basis is 500 eV. In the present work, all geometry structures were fully relaxed until the force on each atom is less than 0.001 eV/Å, and the convergence criteria is 10^{-6} eV for energy. Brillouin zone integration is sampled out by a $(15 \times 15 \times 1)$ k -mesh Monkhorst-Pack grid for relaxation and calculations for electronic properties of single-layer GeS. For optical properties of strained single-layer GeS, we focus on the effects of biaxial strain on the dielectric coefficient, optical absorption coefficient, and electron energy loss spectrum of single-layer GeS. The dielectric coefficients of single-layer GeS are calculated through the Kramer-Kronig transformation and state transitions in its spectrum.

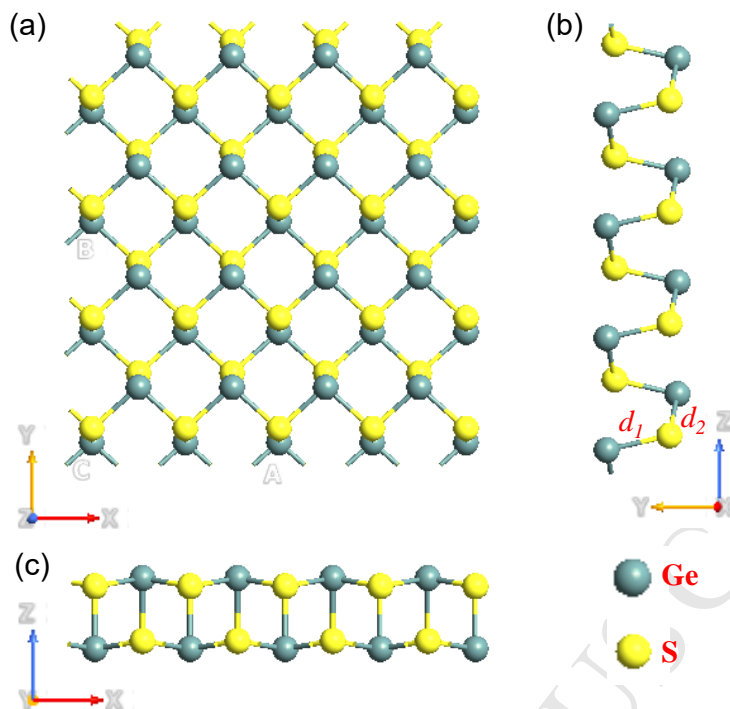


Fig. 1. (Color online) The top view (a), side view (b), and front view (c) of the atomic structure of the single-layer GeS. The yellow and turquoise balls stand respectively for the S and Ge atoms.

3 Results and discussion

The atomic structure of single-layer GeS after relaxation is shown in Fig. 1. One can observe that the single-layer GeS, as shown in Fig. 1, has an orthorhombic structure. The puckered honeycomb lattice of GeS has an anisotropic crystal structure along the armchair and zigzag directions. At that, there is high electric dipole moment along symmetry axis then the dipole moments along one axis can be differed from each other. Hence the dielectric constants are anisotropic as they depend on wave vector direction of an electromagnetic wave in materials (see also Refs. [21, 45, 46]). Our DFT calculations demonstrate that, the lattice parameters of the single-layer GeS are $a = 3.675 \text{ \AA}$, and $b = 4.474 \text{ \AA}$. This result is very close to the available theoretical data [34, 38] and it is in good agreement with experiment value [25]. In addition, our calculations for Ge–S bond lengths d_1 and

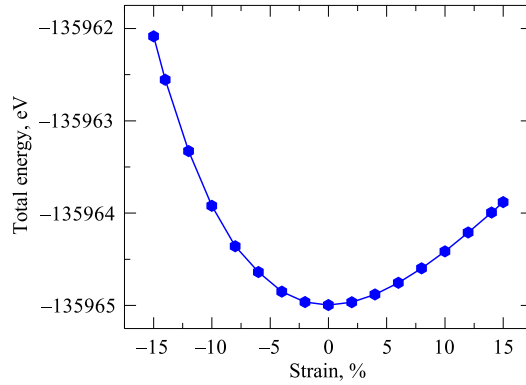


Fig. 2. (Color online) The total energy of single-layer GeS in the presence of the biaxial strain.

d_2 are respectively 4.425 Å and 4.462 Å, which are in good agreement with previous DFT calculations [38]. In the present work, we concentrate on the influence of unique biaxial strain ε_b on electronic properties and optical characteristics of single-layer GeS. Dependence of total energy of single-layer GeS on the ε_b is illustrated in Fig. 2. We can see that the dependence of the total energy of single-layer GeS on the biaxial strain can be illustrated by the parabola. In the large range of biaxial strain, from -15% to 15% , the compression biaxial strain ($\varepsilon < 0$) is a major change in the total energy compared to the tension one.

Our calculations indicate that single-layer GeS is an indirect band gap semiconducting material and its band gap is 1.82 eV at equilibrium as shown in Fig. 3(a). This value is close to the calculated results by DFT with PBE functional [32] and experimental measurement [11]. Accordingly, the valence band maximum (VBM) of single-layer GeS locates at the Γ point or lies on the Y- Γ path while the conduction band minimum (CBM) lies on the Γ -X path [see Fig. 3(a)]. Besides, at the equilibrium state, the minima of the conduction band located at the Γ points are very close to the CBM. Previously, our calculations showed that the mechanical strain is one of the good ways to tune the electronic and optical characters of two-dimensional (2D) materials [5, 47–50]. To consider the electronic properties of

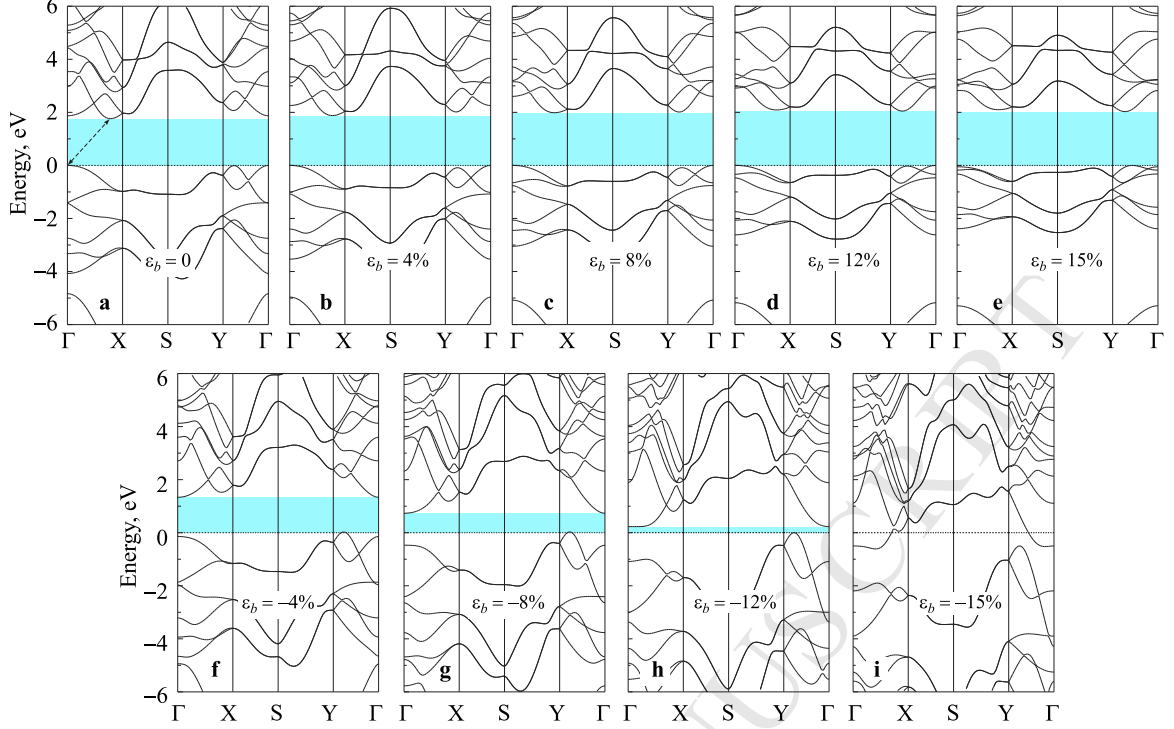


Fig. 3. (Color online) Electronic band structure of single-layer GeS under biaxial strain ε_b : (a) at the equilibrium state ($\varepsilon_b = 0$), (b) $\varepsilon_b = 4\%$, (c) $\varepsilon_b = 8\%$, (d) $\varepsilon_b = 12\%$, (e) $\varepsilon_b = 15\%$, (f) $\varepsilon_b = -4\%$, (g) $\varepsilon_b = -8\%$, (h) $\varepsilon_b = -12\%$, and (i) $\varepsilon_b = -15\%$.

single-layer GeS in the presence of the biaxial strain ε_b , we focus on the calculations of band structure and a band gap of single-layer GeS under biaxial strain ε_b in the large range of elongation from -15% to 15% .

Electronic energy band structure of biaxially strained single-layer GeS is shown in Fig 3. Besides, our calculations indicate that, while the positions of the VBM and CBM of single-layer GeS under biaxial tensile strain ($\varepsilon_b > 0$) is the same as of the case of equilibrium, the position of the CMB changes when the compression strain ($\varepsilon_b < 0$) is applied. Focusing on the influence of the ε_b on the energy gap of single-layer GeS, we found that the influence of tensile strain on the band gap was not large as shown in Fig 4. Meanwhile, the compression strain significantly changes the energy gap of the GeS. Under biaxial compression strain, the band gap of single-layer GeS decreases quickly with increasing $|\varepsilon_b|$ and becomes

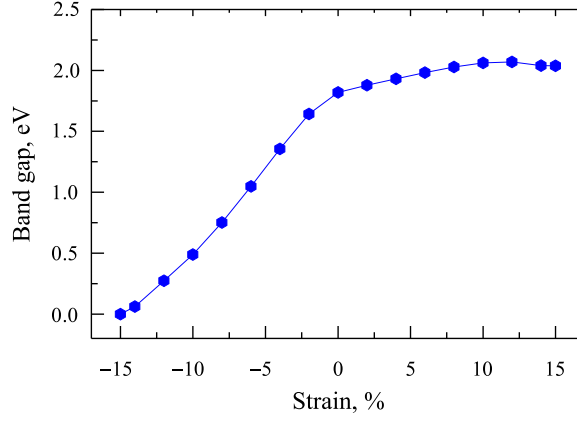


Fig. 4. (Color online) Dependence of band gap of single-layer GeS on the biaxial strain. zero at $\varepsilon_b = -15\%$. It means that the biaxial compression strain can be led to the semiconductor-metal phase transition in single-layer GeS. The band structure of single-layer strained GeS at $\varepsilon_b = -15\%$ is shown in Fig. 3(i). Except at the transition point ($\varepsilon_b = -15\%$), the change in band gap is due to the change of the CBM because the VBM is always at the Fermi level ($E_F = 0$) in the entire investigated a range of biaxial strain from -15% to 15% .

We next consider the effect of biaxial strain on optical properties of single-layer GeS. To calculate the dielectric function $\varepsilon(\omega) = \varepsilon_1(\omega) + i\varepsilon_2(\omega)$, one usually estimates the imaginary part $\varepsilon_2(\omega)$ first by sum of the occupied–unoccupied transitions and then calculates the real part $\varepsilon_1(\omega)$ via the Kramer-Kronig transformation [18,51]:

$$\varepsilon_2^{ij}(\omega) = \frac{4\pi^2 e^2}{Vm^2\omega^2} \sum_{nn'\sigma} \langle kn\sigma | p_i | kn'\sigma \rangle \langle kn'\sigma | p_j | kn\sigma \rangle \times f_{kn}(1 - f_{kn'})\delta(E_{kn'} - E_{kn} - \hbar\omega) \quad (1)$$

and

$$\varepsilon_1(\omega) = 1 + \frac{2}{\pi} P \int_0^\infty \frac{\omega' \varepsilon_2(\omega')}{\omega'^2 - \omega^2} d\omega', \quad (2)$$

where ω is the angular frequency of electromagnetic irradiation, e and m are re-

spectively the charge and mass of electron, V is the unit-cell volume, p is the momentum operator, $|knp\rangle$ is the wave function of a crystal with the wave vector \mathbf{k} , f_{kn} is the Fermi distribution function, and σ is spin which corresponds to the energy eigenvalue E_{kn} . In Fig. 5, we showed the calculated results of the dielectric function parts of single-layer GeS under uniform biaxial strain in the energy range from 0 to 8 eV. We find that the dielectric function parts of GeS dramatically change with energy in the energy domain greater than 3 eV. Similar to analyzed above of the electronic band structure, compression strain has caused many interesting characters when analyzing the optical spectrum. From Fig. 5, we see that the compression strain leads to appear more peaks (compared to the equilibrium state and the tensile strain). This means that there were additional interband transitions when the compression biaxial strain is applied to the single-layer GeS. It is found that the additional structure peaks appear at 4.5 eV in the real and imaginary parts of dielectric functions of the single-layer GeS under compressive biaxial strain, as illustrated in Fig. 5. These additional peaks are mainly dominated by the interband transitions from the top of the valence band below the Fermi level along K- Γ path to the conduction bands 1 and 2 above the Fermi level. This is the consequence of

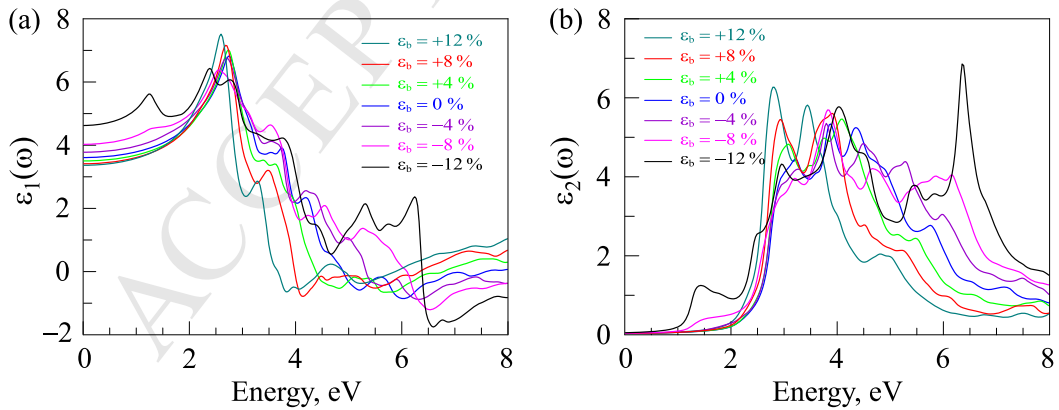


Fig. 5. (Color online) Real $\epsilon_1(\omega)$ (a) and imaginary $\epsilon_2(\omega)$ (b) parts of ϵ of single-layer GeS at different elongations ϵ_b .

transition from the p valence bands of S to the p conduction bands of Ge in the single-layer GeS. Besides, the effect of biaxial strain on the dielectric function is clearly evident in the energy domain greater than 4 eV.

The absorption coefficient $\alpha(\omega)$ can be calculated as [52]

$$\alpha^{ij}(\omega) = \frac{2\omega k^{ij}(\omega)}{c}, \quad (3)$$

where $k^{ij}(\omega)$ is the extinction index which can be expressed as the form

$$k^{ij}(\omega) = \frac{1}{\sqrt{2}} \left[\sqrt{\varepsilon_1^{ij}(\omega)^2 + \varepsilon_2^{ij}(\omega)^2} - \varepsilon_1^{ij}(\omega) \right]^{1/2}. \quad (4)$$

The optical reflectivity $R(\omega)$ can be expressed as the follows

$$R^{ij}(\omega) = \frac{(n^{ij} - 1)^2 + k^{ij2}}{(n^{ij} + 1)^2 - k^{ij2}} = \left| \frac{\sqrt{\varepsilon_1^{ij} + i\varepsilon_2^{ij}} - 1}{\sqrt{\varepsilon_1^{ij} + i\varepsilon_2^{ij}} + 1} \right|^2. \quad (5)$$

Here, the refraction index $n^{ij}(\omega)$ can be written as

$$n^{ij}(\omega) = \frac{1}{\sqrt{2}} \left[\sqrt{\varepsilon_1^{ij}(\omega)^2 + \varepsilon_2^{ij}(\omega)^2} + \varepsilon_1^{ij}(\omega) \right]^{1/2}. \quad (6)$$

Fig. 6 illustrates the absorption coefficient and optical reflectivity of biaxially strained single-layer GeS at different elongations ε_b . As shown in Fig. 6(a), at the equilibrium state ($\varepsilon_b = 0$), the maximum absorption coefficient is at 5.9 eV, i.e., in the

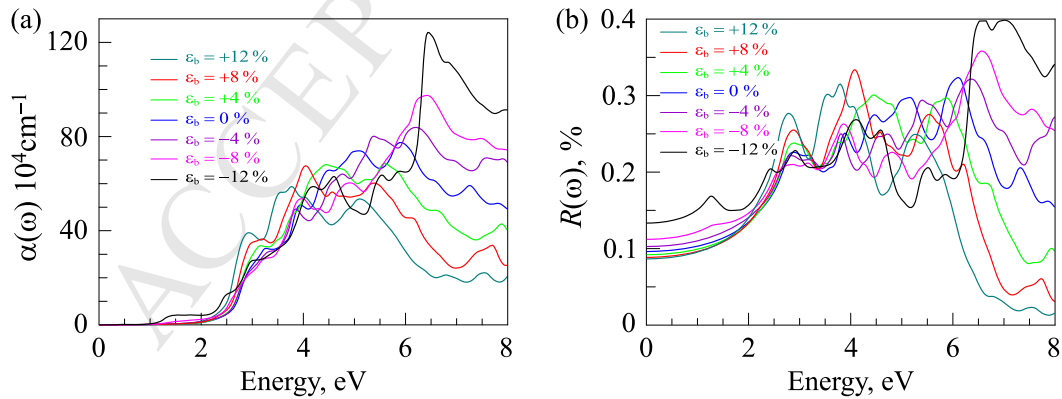


Fig. 6. (Color online) Absorption coefficient $\alpha(\omega)$ (a) and optical reflectivity $R(\omega)$ (b) of biaxially strained single-layer GeS at different elongations ε_b .

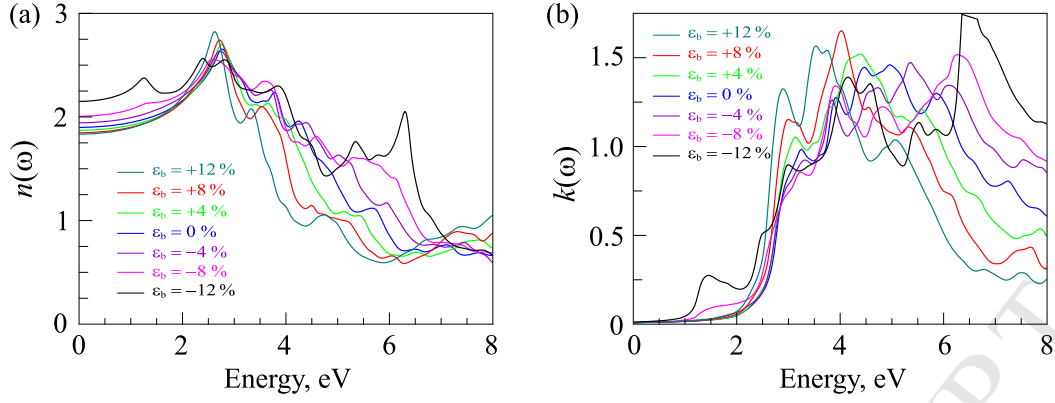


Fig. 7. (Color online) Reflective index $n(\omega)$ (a) and extinction coefficient $k(\omega)$ of single-layer GeS under biaxial strain.

range of the middle ultraviolet lights. Also, we can see that the absorption coefficient of strained single-layer GeS is less fluctuation in the energy range from 0 to 4 eV. In the energy domain greater than 4 eV, the absorption coefficient varies dramatically with the energy. In the range from 5 eV to 8 eV, the absorption coefficient of single-layer GeS depends strongly on the biaxial strain. Our calculations demonstrate that, the absorption coefficient is maximum at 6.1 eV when the single-layer GeS is under the $\varepsilon_b = -8\%$

The reflective index $n(\omega)$ and extinction coefficient $k(\omega)$ of biaxially strained single-layer GeS are shown in Fig. 7. We can see that, both reflective index $n(\omega)$ and extinction coefficient $k(\omega)$ are varies dramatically with energy in the high energy regime. Besides, the biaxial strain ε_b affects strongly on the extinction coefficient $k(\omega)$ in the high energy regime. Among the optical spectra of GeS, we find that dependence of electron energy loss spectrum $L(\omega)$, which is defined by $L(\omega) = -Im(\varepsilon^{-1})^{ij}$, on the energy can be represented by smoother lines compared to other optical parameters. The effect of the biaxial strain ε_b on the $L(\omega)$ is shown in Fig. 8. We can see that, $L(\omega)$ depends strongly on the biaxial strain ε_b , especially in the energy regime greater than 4 eV.

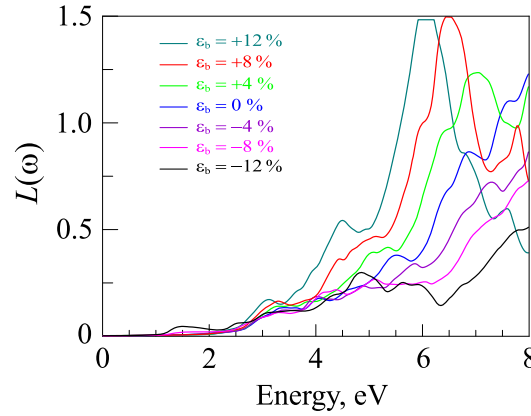


Fig. 8. (Color online) Electron energy loss spectrum $L(\omega)$ of single-layer GeS at different elongations ε_b .

4 Conclusion

In summary, we have studied the influence of biaxial strain ε_b on electronic and optical properties of single-layer GeS using DFT calculations. Our DFT calculated results indicated that the band gap of single-layer GeS depends strongly on the biaxial compression strain ($\varepsilon_b < 0$). The biaxial strain not only causes an indirect-direct band gap transition but also leads to the semiconductor-metal transition in single-layer GeS at large biaxial compression strain ε_b . The optical absorption of single-layer GeS is high in the range of the middle ultraviolet lights, and the effects of the biaxial strain on almost optical spectra are only apparent in energy domain greater than 4 eV. The appearance of the semiconductor-metal transition and the obtained results on the optical properties in the present work may provide additional useful information for the application of GeS in optoelectronic devices.

5 Acknowledgments

This research is funded by the Vietnam National Foundation for Science and Technology Development (NAFOSTED) under Grant Number 103.01-2017.309.

References

- [1] K. S. Novoselov, A. K. Geim, S. V. Morozov, D. Jiang, Y. Zhang, S. V. Dubonos, I. V. Grigorieva, A. A. Firsov, *Science* 306 (2004) 666.
- [2] M. Xu, T. Liang, M. Shi, H. Chen, *Chem. Rev.* 113 (2013) 3766.
- [3] A. K. Geim, I. V. Grigorieva, *Nature* 499 (2013) 419.
- [4] K. Cheng, Y. Guo, N. Han, Y. Su, J. Zhang, J. Zhao, *J. Mater. Chem. C* 5 (2017) 3788.
- [5] H. V. Phuc, N. N. Hieu, B. D. Hoi, L. T. T. Phuong, C. V. Nguyen, *Surf. Sci.* 668 (2018) 23.
- [6] H. V. Phuc, V. V. Ilyasov, N. N. Hieu, C. V. Nguyen, *Vacuum* 149 (2018) 231.
- [7] L. Yi-Hsien, Z. Xin-Quan, Z. Wenjing, C. Mu-Tung, L. Cheng-Te, C. Kai-Di, Y. Ya-Chu, W. J. Tse-Wei, C. Chia-Seng, L. Lain-Jong, L. Tsung-Wu, *Adv. Mater.* 24 (2012) 2320.
- [8] G. Deokar, D. Vignaud, R. Arenal, P. Louette, J.-F. Colomer, *Nanotechnology* 27 (2016) 075604.
- [9] L. Li, Y. Yu, G. J. Ye, Q. Ge, X. Ou, H. Wu, D. Feng, X. H. Chen, Y. Zhang, *Nat. Nanotechnol.* 9 (2014) 372.
- [10] A. H. Woomer, T. W. Farnsworth, J. Hu, R. A. Wells, C. L. Donley, S. C. Warren, *ACS Nano* 9 (2015) 8869.
- [11] D. D. Vaughn, R. J. Patel, M. A. Hickner, R. E. Schaak, *J. Am. Chem. Soc.* 132 (2010) 15170.
- [12] B. Mukherjee, Y. Cai, H. R. Tan, Y. P. Feng, E. S. Tok, C. H. Sow, *ACS Appl. Mater. Interfaces* 5 (2013) 9594.
- [13] C. V. Nguyen, N. N. Hieu, V. V. Ilyasov, *J. Electron. Mater.* 45 (2016) 4038.

- [14] H. S. S. Ramakrishna Matte, A. Gomathi, A. K. Manna, D. J. Late, R. Datta, S. K. Pati, C. N. R. Rao, *Angew. Chem. Int. Ed.* 49 (2010) 4059.
- [15] C. V. Nguyen, N. N. Hieu, N. A. Poklonski, V. V. Ilyasov, L. Dinh, T. C. Phong, L. V. Tung, H. V. Phuc, *Phys. Rev. B* 96 (2017) 125411.
- [16] C. V. Nguyen, N. Hieu, C. A. Duque, D. Khoa, N. Hieu, L. Tung, H. Phuc, *J. Appl. Phys.* 121 (2017) 045107.
- [17] S. Soleimanikahnoj, I. Knezevic, *J. Comput. Electron.* 16 (2017) 568.
- [18] S. Z. Karazhanov, P. Ravindran, A. Kjekshus, H. Fjellvag, B. G. Svensson, *Phys. Rev. B* 75 (2007) 155104.
- [19] M. Wu, S.-H. Wei, L. Huang, *Phys. Rev. B* 96 (2017) 205411.
- [20] R. Fei, W. Kang, L. Yang, Ferroelectricity and phase transitions in monolayer group-IV monochalcogenides, *Phys. Rev. Lett.* 117 (9) (2016) 097601.
- [21] L. Makinistian, E. A. Albanesi, *Phys. Rev. B* 74 (2006) 045206.
- [22] H. Wang, X. Qian, *2D Materials* 4 (2017) 015042.
- [23] C. Chowdhury, S. Karmakar, A. Datta, *J. Phys. Chem. C* 121 (2017) 7615.
- [24] F. Li, X. Liu, Y. Wang, Y. Li, *J. Mater. Chem. C* 4 (2016) 2155.
- [25] T. Yabumoto, *J. Phys. Soc. Jpn.* 13 (1958) 559.
- [26] J. D. Wiley, S. Pennington, E. Schönherr, *Phys. Stat. Sol. (b)* 96 (1979) K37.
- [27] C. Li, L. Huang, G. P. Snigdha, Y. Yu, L. Cao, *ACS Nano* 2 (2012) 8868.
- [28] A. K. Singh, R. G. Hennig, *Appl. Phys. Lett.* 105 (2014) 042103.
- [29] S. Zhang, N. Wang, S. Liu, S. Huang, W. Zhou, B. Cai, M. Xie, Q. Yang, X. Chen, *Nanotechnology* 27 (2016) 274001.

- [30] T. Rangel, B. M. Fregoso, B. S. Mendoza, T. Morimoto, J. E. Moore, J. B. Neaton, *Phys. Rev. Lett.* 119 (2017) 067402.
- [31] A. M. Cook, B. M. Fregoso, F. de Juan, S. Coh, J. E. Moore, *Nat. Commun.* 8 (2017) 14176.
- [32] Z. Ma, B. Wang, L. Ou, Y. Zhang, X. Zhang, Z. Zhou, *Nanotechnology* 27 (2016) 415203.
- [33] S. Demirci, N. Avazli, E. Durgun, S. Cahangirov, *Phys. Rev. B* 95 (2017) 115409.
- [34] L. Xu, M. Yang, S. J. Wang, Y. P. Feng, *Phys. Rev. B* 95 (2017) 235434.
- [35] M. Zhang, Y. An, Y. Sun, D. Wu, X. Chen, T. Wang, G. Xu, K. Wang, *Phys. Chem. Chem. Phys.* 19 (2017) 17210.
- [36] Y. Ma, Y. Dai, M. Guo, L. Yu, B. Huang, *Phys. Chem. Chem. Phys.* 15 (2013) 7098.
- [37] L. Huang, Z. Chen, J. Li, *RSC Adv.* 5 (2015) 5788.
- [38] L. Huang, F. Wu, J. Li, *J. Chem. Phys.* 144 (2016) 114708.
- [39] Y. Xu, H. Zhang, H. Shao, G. Ni, J. Li, H. Lu, R. Zhang, B. Peng, Y. Zhu, H. Zhu, C. M. Soukoulis, *Phys. Rev. B* 96 (2017) 245421.
- [40] Y. Ye, Q. Guo, X. Liu, C. Liu, J. Wang, Y. Liu, J. Qiu, *Chem. Mater.* 29 (2017) 8361.
- [41] L. C. Gomes, A. Carvalho, *Phys. Rev. B* 92 (2015) 085406.
- [42] P. Giannozzi, S. Baroni, N. Bonini, M. Calandra, R. Car, C. Cavazzoni, D. Ceresoli, G. L. Chiarotti, M. Cococcioni, I. Dabo, A. D. Corso, S. de Gironcoli, S. Fabris, G. Fratesi, R. Gebauer, U. Gerstmann, C. Gougoussis, A. Kokalj, M. Lazzeri, L. Martin-Samos, N. Marzari, F. Mauri, R. Mazzarello, S. Paolini, A. Pasquarello, L. Paulatto, C. Sbraccia, S. Scandolo, G. Sclauzero, A. P. Seitsonen, A. Smogunov, P. Umari, R. M. Wentzcovitch, *J. Phys.: Condens. Matter* 21 (2009) 395502.
- [43] J. P. Perdew, K. Burke, M. Ernzerhof, *Phys. Rev. Lett.* 77 (1996) 3865.

- [44] J. P. Perdew, K. Burke, M. Ernzerhof, *Phys. Rev. Lett.* 78 (1997) 1396.
- [45] D. Tan, H. E. Lim, F. Wang, N. B. Mohamed, S. Mouri, W. Zhang, Y. Miyauchi, M. Ohfuchi, K. Matsuda, *Nano Res.* 10 (2) (2017) 546.
- [46] V. M. Agranovich, V. Ginzburg, *Crystal Optics with Spatial Dispersion, and Excitons*, Springer, Berlin, 1984.
- [47] C. V. Nguyen, N. N. Hieu, *Chem. Phys.* 468 (2016) 9.
- [48] N. N. Hieu, H. V. Phuc, V. V. Ilyasov, N. D. Chien, N. A. Poklonski, N. Van Hieu, C. V. Nguyen, *J. Appl. Phys.* 122 (2017) 104301.
- [49] H. V. Phuc, N. N. Hieu, B. D. Hoi, L. T. T. Phuong, N. V. Hieu, C. V. Nguyen, *Superlattices Microstruct.* 112 (2017) 554.
- [50] N. N. Hieu, V. V. Ilyasov, T. V. Vu, N. A. Poklonski, H. V. Phuc, L. T. T. Phuong, B. D. Hoi, C. V. Nguyen, *Superlattices Microstruct.* 115 (2018) 10.
- [51] A. Delin, P. Ravindran, O. Eriksson, J. Wills, *Int. J. Quantum Chem.* 69 (1998) 349–358.
- [52] P. Ravindran, A. Delin, B. Johansson, O. Eriksson, J. M. Wills, *Phys. Rev. B* 59 (1999) 1776.